Stomatal Spacing Safeguards Stomatal Dynamics by Facilitating Guard Cell Ion Transport Independent of the Epidermal Solute Reservoir[1,2][CC-BY]

Maria Papanatsiou, Anna Amtmann, and Michael R. Blatt*

Institute of Molecular Plant Science, School of Biology, University of Edinburgh, Edinburgh EH9 3JR, United Kingdom (M.P.); and Laboratory of Plant Physiology and Biophysics, Institute of Molecular, Cell, and Systems Biology, University of Glasgow, Glasgow G12 8QQ, United Kingdom (M.P., A.A., M.R.B.)

ORCID ID: 0000-0003-1361-4645 (M.R.B.).

Stomata enable gaseous exchange between the interior of the leaf and the atmosphere through the stomatal pore. Control of the pore aperture depends on osmotic solute accumulation by, and its loss from the guard cells surrounding the pore. Stomata in most plants are separated by at least one epidermal cell, and this spacing is thought to enhance stomatal function, although there are several genera that exhibit stomata in clusters. We made use of Arabidopsis (*Arabidopsis thaliana*) stomatal patterning mutants to explore the impact of clustering on guard cell dynamics, gas exchange, and ion transport of guard cells. These studies showed that stomatal clustering in the Arabidopsis *too many mouths* (*tmm1*) mutant suppressed stomatal movements and affected CO_2 assimilation and transpiration differentially between dark and light conditions and were associated with alterations in K^+ channel gating. These changes were consistent with the impaired dynamics of *tmm1* stomata and were accompanied by a reduced accumulation of K^+ ions in the guard cells. Our findings underline the significance of spacing for stomatal dynamics. While stomatal spacing may be important as a reservoir for K^+ and other ions to facilitate stomatal movements, the effects on channel gating, and by inference on K^+ accumulation, cannot be explained on the basis of a reduced number of epidermal cells facilitating ion supply to the guard cells.

Stomata are pores found in the epidermis of most aerial parts of plants and are formed between a specialized pair of cells, the guard cells. Stomata facilitate the uptake of CO_2 at the expense of water vapor release via transpiration (Hetherington and Woodward, 2003). Hence, stomata play a crucial role in the physiology of plants. They permit gaseous exchange between the environment and the inside of the leaf for photosynthesis and, in turn, they influence the water use efficiency and growth of the plant. Mathematical models have suggested that historical changes in the freshwater resources can be attributed to stomatal transpiration, and it has been argued that the manipulation of stomata will be an important factor in ensuring water availability over the next 20 to 30 years (UNESCO World Water Development Report, 2015). Efforts to develop crops with higher water use efficiency through conventional breeding strategies have led to some successes, including the Drysdale wheat (*Triticum aestivum*) variety (Condon et al., 2002). It is likely that further advances will be possible as we gain insights into the physiology of stomata in situ.

The regulation of gas exchange is achieved by controlling the stomatal pore. Stomata respond dynamically to environmental changes, including light quality and intensity, ambient CO_2 concentration, and humidity (Aphalo and Jarvis, 1991; Hetherington and Woodward, 2003; Shimazaki et al., 2007). Stomatal movements result from changes in guard cell volume and turgor and are driven by solute and water fluxes across the plasma membrane and tonoplast of guard cells. In particular, fluxes of the predominant inorganic cation K^+ are mediated by the voltage-dependent inward-rectifying K^+ channels (I_{KIN}), in Arabidopsis (*Arabidopsis thaliana*) by the channel proteins KAT1 and KAT2, during stomatal opening (Blatt and Clint, 1989; Clint and Blatt, 1989; Kwak et al., 2001; Dreyer and Blatt, 2009) and by outward-rectifying K^+ channels (I_{KOUT}), notably GORK in Arabidopsis, during stomatal closure (Blatt and Clint, 1989; Clint and Blatt, 1989; Blatt, 1991; Hosy et al., 2003; Wang et al., 2012).

It has generally been argued that the osmotic solutes required for stomatal movements are provided by the

[1] This work was supported by the M.L. MacIntyre Begonia Trust (Ph.D. studentship to M.P.) and the Biotechnology and Biological Sciences Research Council (grant nos. BB/I024496/1, BB/K015893/1, BB/L001276/1, and BB/M01133X/1 to M.R.B.).

[2] We dedicate this article to the memory of the late Professor Fred Sack, formerly of Ohio State University and the University of British Columbia, and to his generous spirit.

* Address correspondence to michael.blatt@glasgow.ac.uk.

The author responsible for distribution of materials integral to the findings presented in this article in accordance with the policy described in the Instructions for Authors (www.plantphysiol.org) is: Michael R. Blatt (michael.blatt@glasgow.ac.uk).

M.P. carried out the gas-exchange and electrophysiological studies; M.P. and M.R.B. analyzed the data; M.P., A.A., and M.R.B wrote the article.

www.plantphysiol.org/cgi/doi/10.1104/pp.16.00850

surrounding leaf tissues, which act as both a source and sink for ions (Raschke and Fellows, 1971; MacRobbie and Lettau, 1980; Outlaw, 1983; Wilmer and Fricker, 1996; Franks and Farquhar, 2007). For example, previous studies showed that the accumulation of K^+ in *Commelina communis* guard cells was accompanied by its loss from the surrounding epidermal cells during stomatal opening, and the reverse was observed during the closing process (MacRobbie and Lettau, 1980). The presence of epidermal neighboring cells to provide an exchange of osmotic solute also is argued to eliminate the mechanical back pressure from guard cells. Indeed, Franks and Farquhar (2007) have noted the distinct arrangements of stomatal complexes between species and their association with adjacent epidermal cells allowing the ion exchange required for the opening process.

The majority of plant species follow a one-cell spacing rule during epidermal development that leads to the separation of stomata by at least one epidermal cell (Geisler et al., 2000; Peterson et al., 2010; Pillitteri and Dong, 2013). However, there are several genera that diverge from this rule. For instance, stomatal clustering in *Begonia* has been considered to be an adaptation for growth in ecological niches with low water availability (Hoover, 1986; Tang et al., 2002). Even so, no quantitative data are available confirming an advantage of species with stomatal clusters to grow in dry environments. To date, only one study with Arabidopsis transgenic lines has reported on the impact of stomatal clustering in plant physiology, suggesting a negative correlation between gaseous exchange and the degree of clustering (Dow et al., 2014). Those authors speculated that the much-reduced availability of adjacent epidermal cells could explain the altered stomatal behavior in plants with stomatal clusters.

We have revisited the physiological impact of stomatal clustering, making use of the Arabidopsis mutant *too many mouths* (*tmm1*; Yang and Sack, 1995; Geisler et al., 2000) that exhibits stomatal clusters. We find that stomatal clustering of the Arabidopsis *tmm1* mutant affects stomatal behavior. We also provide evidence that this impairment is linked to changes in ion transport at the guard cell plasma membrane and is independent of the presence of neighboring epidermal cells that mediate ionic exchange with the guard cells. These results emphasize the importance of spacing between stomata to ensure proper stomatal behavior and indicate that its impact goes beyond sole mechanical, spatial, or source-sink relations.

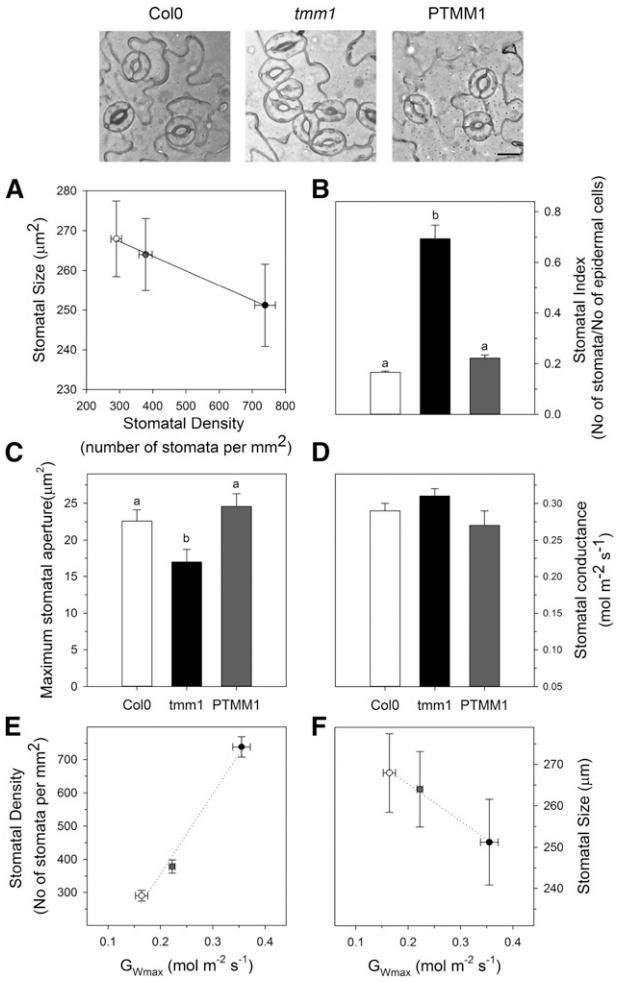

Figure 1. Stomatal characteristics of Arabidopsis lines. The images at top display representative micrographs from the abaxial side of Arabidopsis wild-type (Col-0), *tmm1*, and PTMM1 plants. Bar = 20 μm. A to C, Stomatal patterning was determined from epidermal peels of wild-type (white symbols), *tmm1* (black symbols), and PTMM1 (gray symbols) plants. Graphs represent correlation between stomatal density and stomatal size ($r^2 = 0.99$; A), mean stomatal index (B), and mean maximum stomatal aperture (C). Data are means ± SE of $n > 60$ stomata from three independent experiments. Letters indicate statistical differences among Arabidopsis lines ($P < 0.05$) as determined by the Student-Newman-Keuls test. D, Steady-state diffusional stomatal conductance was measured from Arabidopsis leaves treated with saturating light of 400 μmol m^{-2} s^{-1}. Data are means ± SE of $n = 3$ plants. No significant differences among Arabidopsis lines ($P < 0.05$) were detected. E and F, G_{Wmax} showed a positive correlation with stomatal density (E; $r^2 = 0.98$) and a negative correlation with stomatal size (F; $r^2 = 0.97$). Data are means ± SE of $n > 60$ stomata from three independent experiments.

RESULTS

Stomatal Clustering Affects Maximum Stomatal Conductance

Stomatal patterning was analyzed in epidermal peels from Arabidopsis wild-type Columbia-0 (Col-0), the *tmm1* mutant, and the complementation line PTMM1 (Fig. 1). The mean stomatal density ranged between 290 to 740 stomata per mm^2 for Arabidopsis. The *tmm1* plants showed significantly higher stomatal density compared with wild-type and PTMM1 plants. The lines showed an inverse correlation between stomatal density and size, with smaller stomata being more numerous (Fig. 1A), as has been reported previously (Hunt and Gray, 2009; Doheny-Adams et al., 2012). The differences in the number and size of stomata also were apparent in the stomatal index, which is the ratio of the

number of stomata over the number of nonstomatal cells. The *tmm1* mutant showed a roughly 4-fold greater stomatal index than wild-type and PTMM1 plants (Fig. 1B).

We examined stomatal opening in stomatal clusters by treating epidermal peels with depolarizing buffer (60 mM KCl-MES, pH 6.1; Papanatsiou et al., 2015) under high light intensity for 2 h. Maximum opening of stomatal pores was measured by incorporating the geometry of individual guard cells as well as the whole stoma to calculate the area within the pore, as described previously (Doheny-Adams et al., 2012; Meckel et al., 2007). The wild-type and PTMM1 plants yielded stomatal apertures of 22.6 ± 1.5 and 24.6 ± 1.7 μm^2, respectively (Fig. 1C). By contrast, the stomatal aperture of the *tmm1* mutant was 24% smaller than that of the wild type, yielding values of 16.9 ± 1.7 μm^2.

We also carried out infrared gas analysis at the leaf level to estimate the diffusional stomatal conductance using saturating light as the opening stimulus. In selecting the level of photosynthetic active radiation (PAR), we performed light curves that show the response of the assimilation of CO_2 over different quantum flux densities, ranging from 0 to 800 $\mu mol\ m^{-2}\ s^{-1}$ (Supplemental Fig. S1). The mean diffusional stomatal conductance at saturating light (400 $\mu mol\ m^{-2}\ s^{-1}$) was indistinguishable between plants with single stomata and stomatal clusters (Fig. 1D). We also calculated the theoretical maximum conductance for water vapor (G_{Wmax}) of each line based on the measurements of maximum stomatal aperture as well as the spatial specifications of stomata. G_{Wmax} was positively correlated with the stomatal density (Fig. 1E), whereas it was negatively correlated with stomatal size (Fig. 1F). Both observations were consistent with previous reports (Franks et al., 2009; Franks and Beerling, 2009). We noted that the G_{Wmax} of *tmm1* was greater than that of the plants with single stomata but that measured conductances were indistinguishable among the lines, indicating that the mutant was unable to approach its theoretical maximum as closely as the wild-type and PTMM1 plants.

Spacing between Stomata Is Essential for Stomatal Closure

Evidence for the effects of stomatal clustering on stomatal function is scarce. Only Dow et al. (2014) examined the effects of stomatal clustering and reported the reduced gas exchange and photosynthetic capacity when plants were subjected to different CO_2 concentrations, ranging from 200 to 1,000 $\mu mol\ CO_2\ mol^{-1}$. We carried out complementary measurements, examining the effects of light and dark transitions on CO_2 assimilation and transpiration associated with the dynamics of stomatal movements (Supplemental Fig. S2).

The kinetics of gas-exchange responses upon exposure to light/dark treatments are summarized in Table I and Figure 2. Stomatal clustering in Arabidopsis plants did not influence the kinetics of changes in gas exchange under any light or dark treatment (Table I), but it did affect the steady-state rates of gas exchange (Fig. 2). CO_2 assimilation of *tmm1* appeared lower when plants were subjected to saturating light (400 $\mu mol\ m^{-2}\ s^{-1}$). The *tmm1* plants exhibited a 20% lower maximum rate of CO_2 assimilation, corresponding to a value of 7.8 ± 0.23 $\mu mol\ CO_2\ m^{-2}\ s^{-1}$ compared with 9.3 ± 0.5 $\mu mol\ CO_2\ m^{-2}\ s^{-1}$ in wild-type plants and 9.0 ± 0.1 $\mu mol\ CO_2\ m^{-2}\ s^{-1}$ in PTMM1 plants. No differences between the Arabidopsis lines were observed in the maximum rate of CO_2 assimilation in the photosynthetically limited low-light conditions (70 $\mu mol\ m^{-2}\ s^{-1}$), suggesting that the altered CO_2 assimilation response was dependent on stomatal aperture, in line with conclusions from Dow et al. (2014).

The steady-state rates of transpiration under the two light treatments from the *tmm1* mutant were not substantially different from those of Arabidopsis plants with single stomata, despite the higher stomatal numbers. However, the *tmm1* plants exhibited higher steady-state rates of transpiration in the dark than the plants with single stomata. When the *tmm1* plants were transferred to dark from the low-light regime, the transpiration rate in the dark was 1.21 ± 0.02 $mmol\ m^{-2}\ s^{-1}$ compared with 0.73 ± 0.06 $mmol\ m^{-2}\ s^{-1}$ in the wild type. Similarly, when the plants were transferred from saturating light intensity, the transpiration rate in the dark of *tmm1* was approximately 20% higher than that of plants with single stomata.

To directly assess the impact of stomatal clustering on stomatal closing, we measured stomatal apertures after treatments with the well-established closing stimuli Ca^{2+} and abscisic acid (ABA; Grabov and Blatt, 1998; Eisenach et al., 2012; Papanatsiou et al., 2015). Stomata of wild-type and PTMM1 plants closed to similar extents, whereas stomata of the *tmm1* mutant

Table I. *Half-times of gas-exchange responses in plants with single stomata and stomatal clusters*

Gas-exchange data from Arabidopsis plants under low and saturating light intensity were fitted to nonlinear regression models to extrapolate half-times for CO_2 assimilation, transpiration under light, and transpiration under darkness. Data are presented in minutes. PAR was measured in $\mu mol\ m^{-2}\ s^{-1}$. Data are means ± SE of $n = 3$ plants per genotype. No significant differences among Arabidopsis lines ($P < 0.05$) were detected.

Plant	CO_2 Assimilation		Transpiration under Light		Transpiration under Darkness	
	70 PAR	400 PAR	70 PAR	400 PAR	70 PAR	400 PAR
Col-0	0.2 ± 0.01	2.03 ± 0.67	5.98 ± 0.46	12.62 ± 2.46	4.42 ± 0.89	3.3 ± 1.07
tmm1	0.23 ± 0.001	1.48 ± 0.3	5.81 ± 0.37	14.01 ± 2.65	5.47 ± 1.16	12.7 ± 4.41
PTMM1	0.42 ± 0.1	1.21 ± 0.08	4.74 ± 0.58	11.15 ± 1.18	3.44 ± 0.92	5.71 ± 0.89

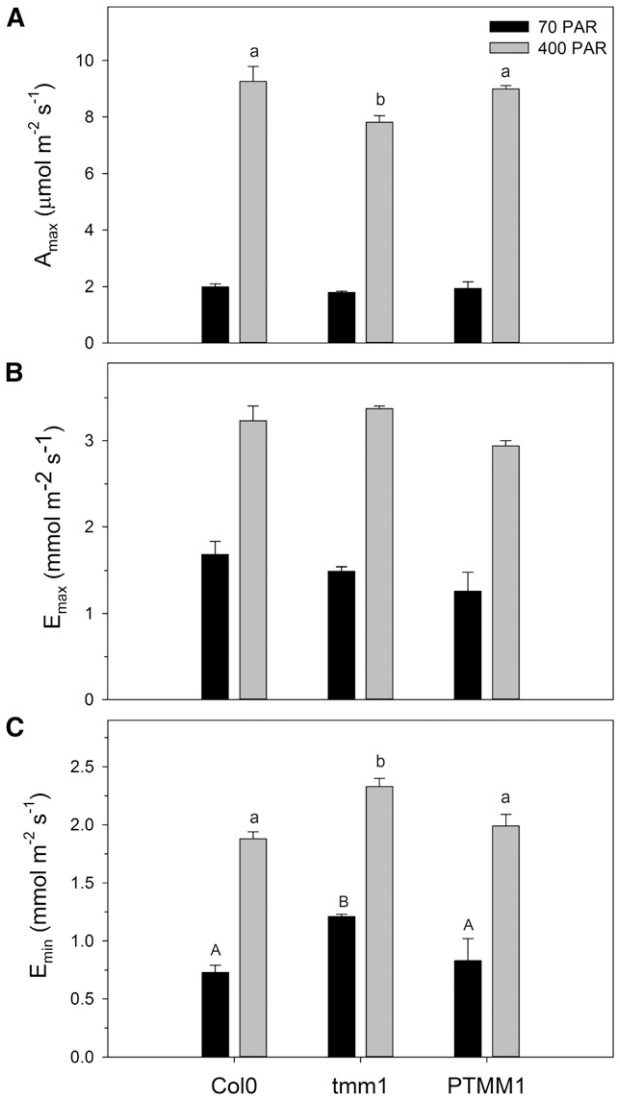

Figure 2. The *tmm1* mutant suppresses gas-exchange responses induced by dark treatment. Steady state gas-exchange triggered by light or darkness is shown. Three-week-old dark-adapted plants were treated with PAR of 70 (black bars) and 400 (gray bars) μmol m^{-2} s^{-1} and then exposed to darkness. Graphs present maximum rates of CO_2 assimilation (A_{max}; A), transpiration under light (E_{max}; B), and transpiration under darkness (E_{min}; C). Data are means ± SE of $n = 3$ plants per species. Letters indicate significant differences among Arabidopsis lines at each light condition ($P < 0.05$) as determined by the Student-Newman-Keuls test.

were impaired in this process (Fig. 3A). The *tmm1* mutant showed a significantly smaller dynamic range of apertures in comparison with wild-type plants following a closing stimulus. We also carried out time-course analysis of stomatal closure in which epidermal peels from Arabidopsis lines were treated with 20 μM ABA and stomata were imaged on a cell-by-cell basis at intervals for 60 min (Fig. 3B). The closing process was attenuated significantly in the *tmm1* mutants, which exhibited 2.5-fold smaller decrease in stomatal aperture than the Arabidopsis lines with single stomata, indicating defects in the movements of stomata in clusters.

Stomatal Clustering Influences Ion Transport in Guard Cells

Stomatal movements depend on the changes in the guard cell turgor pressure and volume that ensue from K^+ fluxes through I_{KIN} and I_{KOUT} at the plasma membrane (Blatt, 1992, 2000a, 2000b; Blatt and Armstrong, 1993). We were interested, therefore, in examining whether ion transport at the guard cell plasma membrane was affected by stomatal clustering. We recorded currents through K^+ channels under voltage clamp from Arabidopsis wild-type, *tmm1*, and PTMM1 guard cells from isolated epidermal peels continuously bathed in solution with a fixed K^+ concentration.

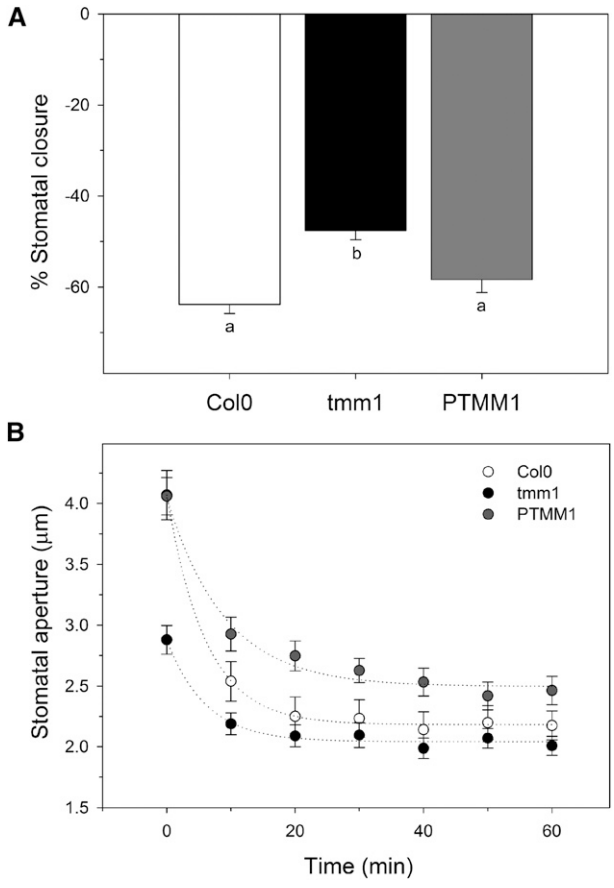

Figure 3. The *tmm1* mutant is defective in stomatal closing. Epidermal peels from wild-type, *tmm1*, and PTMM1 plants were placed in opening buffer and irradiated to ensure maximum stomatal opening before they were treated with buffer containing 6 mM $CaCl_2$ (A) or 20 μM ABA (B) for 60 min to induce stomatal closure. Relative stomatal closing was measured on a cell-by-cell basis. Data are means ± SE of $n > 80$ stomata from three independent experiments. Letters indicate statistical differences between Arabidopsis lines ($P < 0.001$) as determined by the Student-Newman-Keuls test.

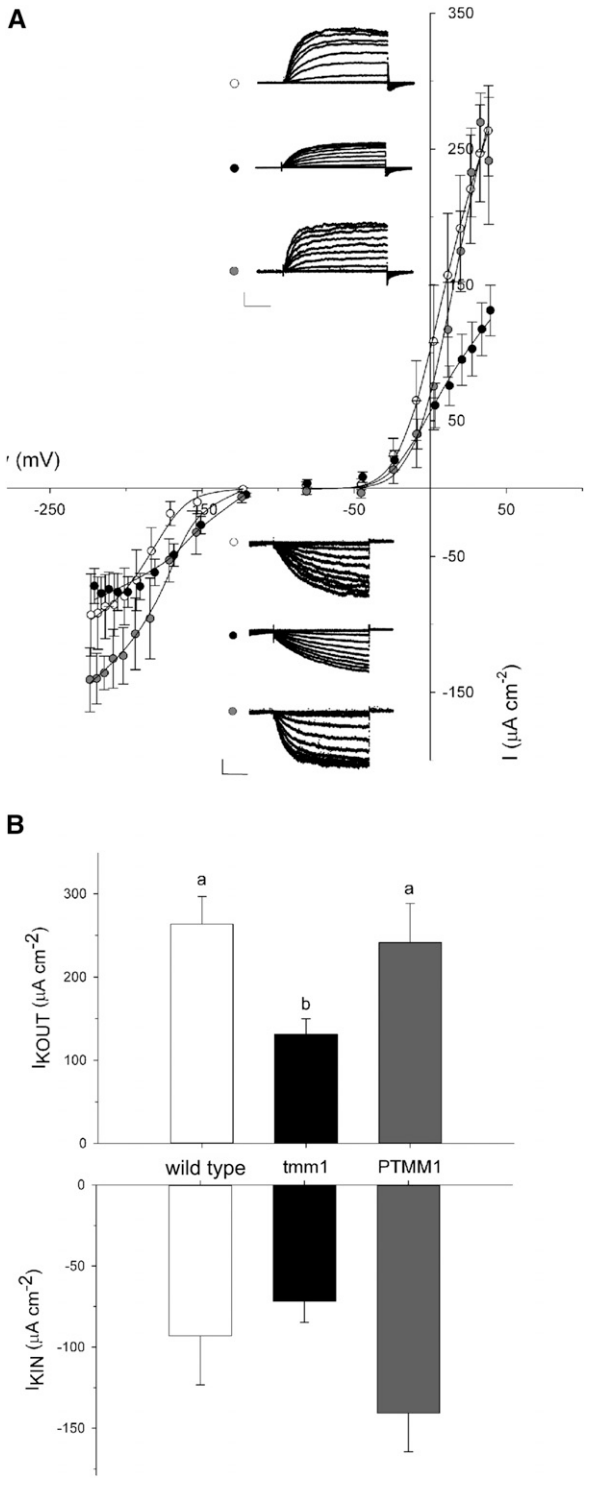

Figure 4. Stomatal clustering alters currents carried through I_{KOUT} and I_{KIN}. A, Currents through I_{KOUT} (top) and I_{KIN} (bottom) recorded under voltage clamp from wild-type (white circles), *tmm1* (black circles), and PTMM1 (gray circles) guard cells. Voltages were clamped from a holding voltage of −100 mV in 6-s steps between −220 and +0 mV and 4-s steps between 0 and +40 mV with 20-mV increments. Data are means ± SE of $n = 5$ guard cells bathed in 5 mM Ca^{2+}-MES buffer, pH 6.1, with 10 mM KCl. The inset shows current traces for I_{KOUT} and I_{KIN} for wild-type, *tmm1*, and PTMM1 plants. Currents are cross-referenced to the current-voltage curves by symbol. Scale bar = 2 s horizontal and 200 μA cm^{-2} vertical. B, Mean current amplitudes for I_{KOUT} (top) and I_{KIN} (bottom) at +40 mV and −220 mV, respectively. Letters indicate statistical differences among Arabidopsis lines ($P < 0.05$) as determined by the Student-Newman-Keuls test.

Figure 4 presents the current traces and average steady-state currents as a function of voltage (current-voltage curves) from guard cells of the Arabidopsis lines. In each case, the currents yielded gating characteristics similar to previous reports (Garcia-Mata et al., 2003; Eisenach et al., 2012; Papanatsiou et al., 2015), albeit with some notable differences in the *tmm1* plants. Voltages positive of −40 mV were marked by strong outward-directed currents, with the current amplitude increasing with increasing voltages, while shifting the voltages to more negative values than −100 mV generated inward-directed currents of increasing amplitude.

To extract the characteristics of changes in the K^+ transport in guard cells found in clusters, we fitted current-voltage curves for each of the currents jointly to a Boltzmann function (see Eq. 4 below) and determined the maximum conductance and gating characteristics of the K^+ channels (Table II). Jointly fitted curves minimize the number of free parameters and allow comparisons between fitting with common parameter values (Honsbein et al., 2009; Wang et al., 2012; Papanatsiou et al., 2015). For I_{KOUT} and I_{KIN}, this analysis yielded statistically and visually satisfactory fittings with the gating charge held in common to give values of 1.9 ± 0.3 and 2.1 ± 0.3, respectively. The maximum conductance for I_{KOUT} from *tmm1* guard cells was reduced by approximately 60% compared with wild-type and PTMM1 cells, whereas no statistically significant alteration was observed for the I_{KIN} among the lines. The amplitude differences aside, we found that the voltage dependence of the I_{KIN} from the *tmm1* mutant was displaced by approximately +30 mV to more positive voltages compared with wild-type Arabidopsis guard cells, indicating that the stomatal clustering also affected the voltage dependence of the gating of the K^+ channels. We carried out quantitative PCR to compare the transcript levels of the plasma membrane H^+-ATPase and three major plasma membrane K^+ channels, the outward-rectifier GORK and the two inward-rectifiers KAT1 and KAT2. This analysis uncovered no substantial difference in transcript levels, suggesting that the alterations in ion transport were not due to altered population sizes or their distributions (Supplemental Fig. S3).

Finally, we made use of the voltage clamp to determine the K^+ content of the guard cells from wild-type and clustered *tmm1* stomata. Tail current analysis provides a direct measure of current reversal and, for any given ensemble of K^+ channels, defines the effective equilibrium voltage that can be used to determine the cytosolic K^+ content. Figure 5A presents current traces and average tail currents for the I_{KOUT} as a function of

Table II. *Gating parameters of I_{KOUT} and I_{KIN}*

g_{max}, Maximum conductance; δ, gating charge; $V_{1/2}$, voltage at which half-maximum activation of channels occurs.Statistical differences were determined after ANOVA and by the Student-Newman-Keuls test for each gating characteristic and among the Arabidopsis lines. *P* values for significant differences are shown for each value.

Plant	I_{KOUT}			I_{KIN}		
	g_{max}	δ	$V_{1/2}$	g_{max}	δ	$V_{1/2}$
	$\mu S\ cm^{-2}$		*mV*	$\mu S\ cm^{-2}$		*mV*
Col-0	2.9 ± 0.1	1.9 ± 0.3	−6 ± 2	0.62 ± 0.02	−1.8 ± 0.3	−177 ± 5
tmm1	1.3 ± 0.07 ($P < 0.001$)		−14 ± 6	0.51 ± 0.01 ($P < 0.05$)		−143 ± 10 ($P < 0.05$)
PTMM1	3 ± 0.2		−1 ± 2	0.75 ± 0.03		−160 ± 5

voltage from guard cells. The point at which no current relaxation was observed defines the reversal voltage. As shown in Figure 5B, the reversal potential was displaced toward more positive values by about 50 mV in the *tmm1* mutant compared with the wild type. From the Nernst equation, the K^+ content of the *tmm1* guard cells was calculated as 54 mM, which is significantly lower than the 199 mM calculated for the wild-type guard cells. Collectively, the results indicate that stomatal clustering affects the K^+ fluxes and the accumulation of K^+ ions in guard cells even under the unrestricted K^+ availability afforded by superfusion with millimolar concentrations in electrophysiological experiments.

DISCUSSION

Substantial evidence shows that stomatal density affects gas exchange, which, in turn, translates to assimilation rates and water use efficiency in plants (Schlüter et al., 2003; Franks et al., 2009; Lawson, 2009; Yoo et al., 2010; Fanourakis et al., 2011; Drake et al., 2013; Tanaka et al., 2013). Only recently has attention turned to questions of the spacing of stomata on the leaf surface and its implications for environmental physiology and adaptation. The stomata of most plants occur singly, one over each substomatal cavity within the leaf mesophyll layer, and are separated by at least one pavement cell within the leaf epidermis. However, in a few plant species, stomata are found to cluster naturally in groups of two or more over a substomatal cavity and may be separated by a narrow wedge only of a pavement cell. Mutants, too, are known in which stomata develop in clusters, often without a separating pavement cell. To date, a single study has shown that Arabidopsis mutants with a high degree of clustering show reductions in gas exchange and are impaired in their capacity for carbon assimilation (Dow et al., 2014). However, until now, no information has been forthcoming on the mechanisms underlying these differences.

We examined the physiology of Arabidopsis and its *tmm1* mutant, which develops clusters without intervening pavement cells (Yang and Sack, 1995; Geisler et al., 2000). These studies compared the gas-exchange characteristics as well as the dynamics of stomatal movements. Additionally, we used voltage clamp analysis to assess the capacities for K^+ flux and to compare the K^+ contents in the Arabidopsis lines. Like Dow et al. (2014), we found that clustering in the Arabidopsis *tmm1* mutant compromises carbon assimilation and stomatal closure. Our studies go further to show that the effects in the mutant are largely a consequence of a reduced dynamic range for stomatal movement and that they are associated with decreases in both the capacity for K^+ flux and the K^+ content of the guard cells. Most interestingly, the differences in stomatal behavior cannot be understood on the basis of channel transcript levels (Supplemental Fig. S3) or solely on the availability of K^+ for exchange with the apoplast and surrounding cells, since the electrophysiological experiments were carried out with isolated epidermal peels in unconstrained K^+ concentration. In addition, the isolation of epidermal peels results in the complete destruction of epidermal cells. Thus, we conclude that spacing between stomata may be important for stomatal function but that the effects on gas-exchange kinetics, suppressed K^+ channel activities, and K^+ content in guard cells of the Arabidopsis *tmm1* mutant are clearly independent of any source-sink relations with the surrounding epidermal cell layer.

Gas Exchange and Stomatal Patterning

It is well documented that stomatal density across dicotyledonous species is balanced against stomatal size and that reducing stomatal size is an important strategy to facilitate stomatal dynamics without increasing the evaporative area of the leaf (Drake et al., 2013). Reducing the size of the guard cells surrounding the stomatal pore has the effect of increasing the ratio of membrane surface area to guard cell volume. Provided that the density of membrane transporters per unit of surface area is nearly constant, a decrease in guard cell size can be expected to accelerate the solute flux per unit of volume proportionally, thereby allowing for faster responses to environmental transients. This strategy is well documented in studies of Arabidopsis (Schlüter et al., 2003; Tanaka et al., 2013) and other plant species (Franks and Farquhar, 2007; Drake et al., 2013; Lawson and Blatt, 2014) and is consistent with mathematical models that take into account the geometry of guard

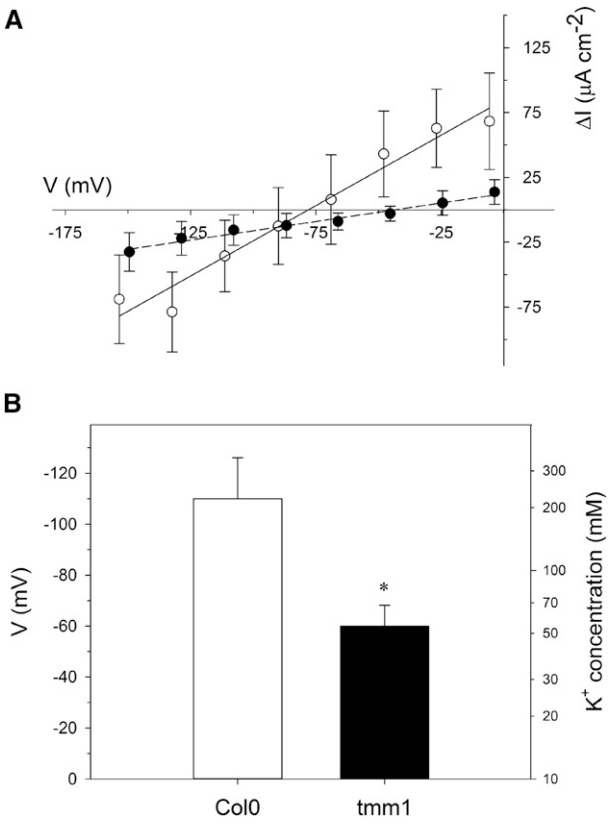

Figure 5. Stomatal clustering alters the cytosolic K^+ content of guard cells. A, Currents through I_{KOUT} recorded under voltage clamp from wild-type (white circles) and *tmm1* (black circles) guard cells. Voltages were clamped from a holding voltage of +50 mV in 5-s steps between −220 and +40 mV. Data are means ± SE of $n = 5$ guard cells bathed in 5 mM Ca^{2+}-MES buffer, pH 6.1, with 10 mM KCl. B, Reversal potential of I_{KOUT} as depicted from the tail current analysis. Decrease in voltage steps led to a negative reversal potential around −110 ± 16 mV for wild-type plants, whereas stomatal clustering of the *tmm1* mutant shifted the reversal potential to a more positive value of −58 mV ± 9 mV. From the Nernst equation, the K^+ concentrations of wild-type and *tmm1* guard cells were calculated as 199 and 54 mM, respectively. The asterisk indicates a statistical difference as determined by Student's *t* test ($P < 0.05$).

cells and the guard cell complex (Doheny-Adams et al., 2012; Dow et al., 2014) as well as membrane transport (Chen et al., 2012; Wang et al., 2012; Lawson and Blatt, 2014). In general, such analysis assumes the physical and spatial independence of each stoma and its positioning over a substomatal cavity.

Our data pointed to a mismatch between measured stomatal conductance and the theoretical maximum stomatal conductance of the *tmm1* mutant (Fig. 1). This finding indicates that the presence of epidermal cells between stomata is crucial to allow stomatal opening and underlines the importance of spacing between stomata. Dow et al. (2014) proposed that the decreased CO_2 assimilation rates in plants with clustered stomata might depend on structural misplacement of stomata over mesophyll tissue. Although we cannot exclude this interpretation, we found that stomata from isolated epidermal peels of *tmm1* failed to open when exposed to opening stimuli (Fig. 1C), suggesting that stomatal impairment in the *tmm1* mutant is not dependent on the substomatal cavity or the underlying photosynthetic tissue. More importantly, we identified that the transpiration rate of *tmm1* plants in the dark was higher (Fig. 2C) and that their response to closing stimuli was attenuated (Fig. 3), indicating a dependence on stomatal aperture rather than on leaf structure. Why assimilation was affected despite the lack of effect on transpiration in the light is puzzling. One possible explanation is that the *tmm1* mutant additionally targets tissue development or function independent of the stomata, which, in turn, might influence water flux through the plant.

The *tmm1* Mutant Affects K^+ Channel Activity and K^+ Content

Of our findings, the most surprising were of alterations in K^+ channel activities and of decreases in the K^+ contents of clustered guard cells in the Arabidopsis *tmm1* mutant (Figs. 4 and 5). Stomatal movements depend on changes in turgor, which is driven largely by the transport of osmotically active solutes and water across the plasma membrane of the guard cells (Blatt, 2000a, 2000b; Franks and Farquhar, 2007). Potassium makes up by far the largest fraction of the inorganic osmotica, and its transport often leads to changes of whole-cell K^+ concentrations from 150 to 400 mM between the closed and open states of the guard cell, respectively (Blatt, 2000a, 2000b; MacRobbie, 1998; Hills et al., 2012; Chen et al., 2012). Guard cells are packed together in the *tmm1* mutant, however, implying a need for substantially greater solute accumulation to drive stomatal opening. The surrounding epidermal or subsidiary cells are thought to serve as a source for K^+ and other ions during stomatal opening and as a sink for the same ions when stomata close (Raschke and Fellows, 1971; MacRobbie and Lettau, 1980; Outlaw, 1983; Franks and Farquhar, 2007). MacRobbie and Lettau (1980) used K^+-sensitive microelectrodes to demonstrate that the K^+ content in the epidermal cells of *C. communis* was reduced from between 180 and 300 mM to 80 mM when the nearby stomata opened, consistent with solute uptake by the guard cells from adjacent subsidiary cells (Penny and Bowling, 1974). However, when isolated in epidermal peels and superfused with solution containing millimolar KCl, any source-sink relations between guard cells and the surrounding epidermis are short-circuited by the nearly infinite volume of the buffer solution. As a consequence, we can rule out any effects associated with epidermal cell placement or their presence as a source of osmoticum and can eliminate any dependency of guard cells for ionic exchange on these neighboring cells. Yet, we observed that the ensemble conductances of both K^+ channels (Fig. 4) and the low K^+ concentrations indicated by tail current

analysis (Fig. 5) were reduced in the *tmm1* mutant. Nor can the effects on the K^+ current be understood as the result of the reduced K^+ content or gene expression (Pilot et al., 2003a; Sutter et al., 2007; Eisenach et al., 2012, 2014). Analysis of the I_{KIN}, especially, showed a substantial shift in the voltage dependence for channel gating, which is independent of cytosolic K^+ concentration (Wilmer and Fricker, 1996; Hills et al., 2012), and no appreciable difference in K^+ channel expression was observed compared with the wild type. The obvious conclusion from these findings is that the *tmm1* mutant affects the channels via posttranslational regulation of their activities. Such control may well arise from the pleiotropic changes in protein kinase and phosphatase signal cascades or more directly through alterations in metabolism that lead to changes in cytosol-free [Ca^{2+}] and pH that modulate these channels, as has been demonstrated for the *slac1* Cl^- channel mutant of Arabidopsis (Wang et al., 2012). Regardless of the final explanation, it is clear that the effects of stomatal clustering are not a simple consequence of the physical spacing of the stomata within the epidermis or their placement in relation to the underlying mesophyll cells.

MATERIALS AND METHODS

Plant Material and Growth Conditions

Arabidopsis (*Arabidopsis thaliana*) Col-0-*gl1* wild-type, *tmm1* mutant, and PTMM1 complementation line (pTMM:TMM1-GFP complementation *tmm1*; Bhave et al., 2009) seeds were obtained from F.D. Sack (University of British Columbia). Plants were grown under 70 μmol m^{-2} s^{-1} light in long-day conditions (16/8 h of light/dark), 22°C/18°C (light/dark) temperature, and 60%/70% (light/dark) relative humidity, except for stomatal assays that were carried out with plants grown in short-day conditions (8/16 h of light/dark). Chemicals were reagent grade from Sigma-Aldrich.

Gas Exchange

Gas exchange was carried out using the LI-COR 6400 XT Infrared Gas Analyzer (LICOR Biosciences) and whole-plant Arabidopsis chamber (LI-COR 6400-17). Pots of Arabidopsis were sealed with cling film to prevent any water vapor and CO_2 diffusion from the soil. All measurements were carried out at 22°C, 60% relative humidity, and 390 μg mL^{-1} CO_2. Gas-exchange responses were measured using an integrated light source (LI-COR 6400-18) after plant materials were adapted to dark for 1.5 h. At least three plants per genotype were measured on different days at the same time of the diurnal cycle. Arabidopsis plants were normalized to the whole rosette area using ImageJ version 1.43u (http://rsb.info.nih.gov/ij; Rasband and Bright, 1995).

Stomatal Assays

Stomatal pattern and stomatal aperture measurements were carried out using epidermal peels isolated as described before (Wang et al., 2012). Images were recorded by digital photomicrography using a Zeiss Axiovert 200 microscope with LD Achroplan 40×/NA0.75 and Planapo 20×/0.80 objectives and an AxioCam HRc digital camera (Zeiss).

Stomatal apertures were recorded from epidermal peels following preincubations in depolarizing buffer (5 mM MES-NaOH, pH 6.15, and 60 mM KCl) for 2 h under 100 μmol m^{-2} s^{-1} light to fully open stomata (Papanatsiou et al., 2015). After imaging, epidermal peels were incubated for 5 min in depolarizing buffer supplemented with 20 μM fluorescein diacetate and examined for fluorescence to confirm vitality. Only stomata that showed fluorescence under confocal microscopy were analyzed further.

Maximum stomatal aperture (a_{max}) was estimated as

$$a_{\max} = \pi W_a L_a / 4 \quad (1)$$

where W_a is the aperture width and L_a is the aperture length. Stomatal size (S_s) was obtained as

$$S_s = \pi W_s L_s / 4\text{-}a_{\max} \quad (2)$$

where W_s is the stoma width and L_s is the stoma length. The theoretical G_{Wmax} was calculated as described by Franks et al. (2009) as

$$G_{W\max} = d S_D a_{\max} \Big/ v\left[l\pi \Big/ 2(a_{\max}/\pi)^{0.5}\right] \quad (3)$$

where d is the diffusivity of water vapor in air (m^2 s^{-1}), v is the molar volume of air at 1 atm and 22°C (m^3 mol^{-1}), S_D is stomatal density (m^{-2}), and l is the pore depth, estimated as the width of fully inflated guard cell.

Stomatal closure was initiated after guard cells were fully open by superfusion with 10 mM MES-KCl, pH 6.1, supplemented with 6 mM $CaCl_2$ or 20 μM ABA. Measurements were carried out on a cell-by-cell basis, and results are reported as means ± SE of $n > 80$ stomata.

Guard Cell Electrophysiology

Currents were recorded under two-electrode voltage clamp using Henry's EP software (Y-Science; http://www.psrg.org.uk). Microelectrodes were constructed to give tip resistances of 300 to 500 MΩ for Arabidopsis impalements, and they were filled with 200 mM K^+ acetate, pH 7.5, to minimize interference arising from anion leakage from the microelectrode (Blatt and Slayman, 1983; Blatt, 1987; Wang and Blatt, 2011). Electrolyte-filling solutions also were equilibrated against the resin-bound Ca^{2+} buffer BAPTA (Ca^{2+} sponge; Invitrogen) to avoid Ca^{2+} loading of the cytosol from the microelectrode. Arabidopsis guard cells from isolated epidermal peels were pretreated with depolarizing buffer and light of 150 μmol m^{-2} s^{-1} to subsequently record K^+ channel currents in bathing solution of 5 mM Ca^{2+}-MES, pH 6.1, supplemented with 10 mM KCl. Current and voltage under clamp were recorded using a set of μP electrometer amplifiers (WyeScience) with an input impedance of greater than 5×10^{11} Ω (Blatt, 1987). Recordings were typically obtained by clamping in cycles with a holding voltage of 2 s at −100 mV and 6-s steps either to voltages from −120 to −240 mV for currents from I_{KIN} or voltages from −80 to +40 mV for currents from I_{KOUT}. Recordings were corrected for background currents determined as the instantaneous current recorded on stepping from the holding voltage, much as described previously (Blatt, 1987; Wang et al., 2012; Papanatsiou et al., 2015).

Current-voltage curves were fitted by joint, nonlinear least squares and the Marquardt-Levenberg algorithm using a Boltzmann function of the form

$$I = G_{max}(V\text{-}E_K) \Big/ \left(1 + e^{\delta z F(V - V_{1/2})/RT}\right) \quad (4)$$

where g_{max} is the maximum conductance, V is the membrane voltage, E_K is the equilibrium voltage for K^+, $V_{1/2}$ is the voltage at which half-maximum activation of channels occurs, z is the ionic valence, δ is the gating charge, and F, R, and T have their usual meanings. Fitting current-voltage curves with the Boltzmann function results in the determination of δ, which describes the apparent sensitivity of current (I) to a change in membrane voltage, and $V_{1/2}$, which defines the midpoint voltage characteristic of this voltage sensitivity.

Tail current analysis was used to estimate the cytosolic concentration of K^+. For this purpose, the membrane was clamped in cycles with a holding voltage of 5 s at +50 mV followed by steps to voltages between +30 and −120 mV. The relaxation amplitudes were plotted as a function of clamp voltage to identify the reversal voltage, at which no current relaxation was seen. This voltage was used as the equilibrium voltage for the K^+ channel, and the cytosolic K^+ concentration was then calculated from the Nernst equation and the known external K^+ concentration as

$$[K^+]_{in} = [K^+]_{out} \Big/ e^{zFE_x/RT} \quad (5)$$

where E_x is the voltage at which the current crosses the voltage axis.

Gene Expression Analysis

Total RNA was extracted from mature leaves of 3-week-old plants grown in long-day conditions, and transcript levels were determined by quantitative PCR,

as described previously (Wang et al., 2012). Specific primers were designed (Wang et al., 2012) for the plasma membrane H^+-ATPase AHA1 (Lopez-Marques et al., 2004) and the K^+ channels KAT1 (At5g46240), KAT2 (At4g18290), and GORK (At5g37500; Hosy et al., 2003; Pilot et al., 2003b). The *TUB9* tubulin (At4g20890) gene (Gutierrez et al., 2008) served as a constitutive control.

Data and Statistical Analyses

Data analysis and curve fitting were carried out using SigmaPlot 12 (Systat Software). Statistical significances were determined using one-way ANOVA and Student's t test at $P < 0.05$.

Accession Numbers

Sequence data from this article can be found in the GenBank/EMBL data libraries under accession number BT005892.

Supplemental Data

The following supplemental materials are available.

Supplemental Figure S1. Effect of photosynthetic radiation on CO_2 assimilation.

Supplemental Figure S2. Time series of gas-exchange responses from Arabidopsis plants.

Supplemental Figure S3. Transcript levels of major plasma membrane transport genes in Arabidopsis lines.

Received May 27, 2016; accepted July 9, 2016; published July 11, 2016.

LITERATURE CITED

Aphalo J, Jarvis PG (1991) Do stomata respond to relative humidity!? Plant Cell Environ **14:** 127–132

Bhave NS, Veley KM, Nadeau JA, Lucas JR, Bhave SL, Sack FD (2009) TOO MANY MOUTHS promotes cell fate progression in stomatal development of Arabidopsis stems. Planta **229:** 357–367

Blatt M, Armstrong F (1993) K^+ channels of stomatal guard cells: abscisic acid-evoked control of the outward rectifier mediated by cytoplasmic pH. Planta **191:** 330–341

Blatt MR (1987) Electrical characteristics of stomatal guard cells: the ionic basis of the membrane potential and the consequence of potassium chlorides leakage from microelectrodes. Planta **170:** 272–287

Blatt MR (1991) Ion channel gating in plants: physiological implications and integration for stomatal function. J Membr Biol **124:** 95–112

Blatt MR (1992) K^+ channels of stomatal guard cells: characteristics of the inward rectifier and its control by pH. J Gen Physiol **99:** 615–644

Blatt MR (2000a) Ca^{2+} signalling and control of guard-cell volume in stomatal movements. Curr Opin Plant Biol **3:** 196–204

Blatt MR (2000b) Cellular signaling and volume control in stomatal movements in plants. Annu Rev Cell Dev Biol **16:** 221–241

Blatt MR, Clint GM (1989) Mechanisms of fusicoccin action: kinetic modification and inactivation of K^+ channels in guard cells. Planta **178:** 509–523

Blatt MR, Slayman CL (1983) KCl leakage from microelectrodes and its impact on the membrane parameters of a nonexcitable cell. J Membr Biol **72:** 223–234

Chen ZH, Hills A, Baetz U, Amtmann A, Lew VL, Blatt MR (2012) Systems dynamic modeling of the stomatal guard cell predicts emergent behaviors in transport, signaling, and volume dontrol. Plant Physiol **159:** 1235–1251

Clint GM, Blatt MR (1989) Mechanisms of fusicoccin action: evidence for concerted modulations of secondary K^+ transport in a higher plant cell. Planta **178:** 495–508

Condon AG, Richards RA, Rebetzke GJ, Farquhar GD (2002) Improving intrinsic water-use efficiency and crop yield. Crop Science **42:** 122–131

Doheny-Adams T, Hunt L, Franks PJ, Beerling DJ, Gray JE (2012) Genetic manipulation of stomatal density influences stomatal size, plant growth and tolerance to restricted water supply across a growth carbon dioxide gradient. Philos Trans R Soc Lond B Biol Sci **367:** 547–555

Dow GJ, Berry JA, Bergmann DC (2014) The physiological importance of developmental mechanisms that enforce proper stomatal spacing in Arabidopsis thaliana. New Phytol **201:** 1205–1217

Drake PL, Froend RH, Franks PJ (2013) Smaller, faster stomata: scaling of stomatal size, rate of response, and stomatal conductance. J Exp Bot **64:** 495–505

Dreyer I, Blatt MR (2009) What makes a gate? The ins and outs of Kv-like K^+ channels in plants. Trends Plant Sci **14:** 383–390

Eisenach C, Chen ZH, Grefen C, Blatt MR (2012) The trafficking protein SYP121 of Arabidopsis connects programmed stomatal closure and K^+ channel activity with vegetative growth. Plant J **69:** 241–251

Eisenach C, Papanatsiou M, Hillert EK, Blatt MR (2014) Clustering of the K^+ channel GORK of Arabidopsis parallels its gating by extracellular K^+. Plant J **78:** 203–214

Fanourakis D, Carvalho SM, Almeida DP, Heuvelink E (2011) Avoiding high relative air humidity during critical stages of leaf ontogeny is decisive for stomatal functioning. Physiol Plant **142:** 274–286

Franks PJ, Beerling DJ (2009) Maximum leaf conductance driven by CO_2 effects on stomatal size and density over geologic time. Proc Natl Acad Sci USA **106:** 10343–10347

Franks PJ, Drake PL, Beerling DJ (2009) Plasticity in maximum stomatal conductance constrained by negative correlation between stomatal size and density: an analysis using Eucalyptus globulus. Plant Cell Environ **32:** 1737–1748

Franks PJ, Farquhar GD (2007) The mechanical diversity of stomata and its significance in gas-exchange control. Plant Physiol **143:** 78–87

Garcia-Mata C, Gay R, Sokolovski S, Hills A, Lamattina L, Blatt MR (2003) Nitric oxide regulates K^+ and Cl^- channels in guard cells through a subset of abscisic acid-evoked signaling pathways. Proc Natl Acad Sci USA **100:** 11116–11121

Geisler M, Nadeau J, Sack FD (2000) Oriented asymmetric divisions that generate the stomatal spacing pattern in *Arabidopsis* are disrupted by the *too many mouths* mutation. Plant Cell **12:** 2075–2086

Grabov A, Blatt MR (1998) Membrane voltage initiates Ca^{2+} waves and potentiates Ca^{2+} increases with abscisic acid in stomatal guard cells. Proc Natl Acad Sci USA **95:** 4778–4783

Gutierrez L, Mauriat M, Guenin S, Pelloux J, Lefebvre JF, Louvet R, Rusterucci C, Moritz T, Guerineau F, Bellini C, Van Wuytswinkel O (2008) The lack of a systematic validation of reference genes: a serious pitfall undervalued in reverse transcription-polymerase chain reaction (RT-PCR) analysis in plants. Plant Biotechnol **6:** 609–618

Hetherington AM, Woodward FI (2003) The role of stomata in sensing and driving environmental change. Nature **424:** 901–908

Hills A, Chen ZH, Amtmann A, Blatt MR, Lew VL (2012) OnGuard, a computational platform for quantitative kinetic modeling of guard cell physiology. Plant Physiol **159:** 1026–1042

Honsbein A, Sokolovski S, Grefen C, Campanoni P, Pratelli R, Paneque M, Chen Z, Johansson I, Blatt MR (2009) A tripartite SNARE-K^+ channel complex mediates in channel-dependent K^+ nutrition in *Arabidopsis*. Plant Cell **21:** 2859–2877

Hoover WS (1986) Stomata and stomatal clusters in Begonia: ecological response in two Mexican species. Biotropica **18:** 16–21

Hosy E, Vavasseur A, Mouline K, Dreyer I, Gaymard F, Porée F, Boucherez J, Lebaudy A, Bouchez D, Very AA, et al (2003) The Arabidopsis outward K^+ channel GORK is involved in regulation of stomatal movements and plant transpiration. Proc Natl Acad Sci USA **100:** 5549–5554

Hunt L, Gray JE (2009) The signaling peptide EPF2 controls asymmetric cell divisions during stomatal development. Curr Biol **19:** 864–869

Kwak JM, Murata Y, Baizabal-Aguirre VM, Merrill J, Wang M, Kemper A, Hawke SD, Tallman G, Schroeder JI (2001) Dominant negative guard cell K^+ channel mutants reduce inward-rectifying K^+ currents and light-induced stomatal opening in Arabidopsis. Plant Physiol **127:** 473–485

Lawson T (2009) Guard cell photosynthesis and stomatal function. New Phytol **181:** 13–34

Lawson T, Blatt MR (2014) Stomatal size, speed, and responsiveness impact on photosynthesis and water use efficiency. Plant Physiol **164:** 1556–1570

Lopez-Marques RL, Schiott M, Jakobsen MK, Palmgren MG (2004) Structure, function and regulation of primary H^+ and Ca^{2+} pumps. *In* MR Blatt, ed, Membrane Transport in Plants, Annual Plant Reviews, Vol 15. Blackwell Publishers, Oxford, UK, pp 72–104

MacRobbie EA (1998) Signal transduction and ion channels in guard cells. Philos Trans R Soc Lond B Biol Sci **353:** 1475–1488

MacRobbie EAC, Lettau J (1980) Membrane biology potassium content and aperture in "intact" stomatal and epidermal cells of Commelina communis L. J Membr Biol **256:** 249–256

Meckel T, Gall L, Semrau S, Homann U, Thiel G (2007) Guard cells elongate: relationship of volume and surface area during stomatal movement. Biophys J **92:** 1072–1080

Outlaw WH (1983) Current concepts on the role of potassium in stomatal movements. Physiol Plant **59:** 302–311

Papanatsiou M, Scuffi D, Blatt MR, García-Mata C (2015) Hydrogen sulfide regulates inward-rectifying K^+ channels in conjunction with stomatal closure. Plant Physiol **168:** 29–35

Penny MG, Bowling DJ (1974) A study of potassium gradients in the epidermis of intact leaves of Commelina communis L. in relation to stomatal opening. Planta **119:** 17–25

Peterson KM, Rychel AL, Torii KU (2010) Out of the mouths of plants: the molecular basis of the evolution and diversity of stomatal development. Plant Cell **22:** 296–306

Pillitteri LJ, Dong J (2013) Stomatal development in Arabidopsis. The Arabidopsis Book **11:** e0162, doi/10.1199/tab.0162

Pilot G, Gaymard F, Mouline K, Chérel I, Sentenac H (2003a) Regulated expression of Arabidopsis shaker K^+ channel genes involved in K^+ uptake and distribution in the plant. Plant Mol Biol **51:** 773–787

Pilot G, Pratelli R, Gaymard F, Meyer Y, Sentenac H (2003b) Five-group distribution of the Shaker-like K^+ channel family in higher plants. J Mol Evol **56:** 418–434

Rasband W, Bright D (1995) NIH IMAGE - A public domain image-processing program for the Macintosh. Microbeam Analysis **4:** 137–149

Raschke K, Fellows MP (1971) Stomatal movement in Zea mays: shuttle of potassium and chloride between guard cells and subsidiary cells. Planta **101:** 296–316

Schlüter U, Muschak M, Berger D, Altmann T (2003) Photosynthetic performance of an Arabidopsis mutant with elevated stomatal density (sdd1-1) under different light regimes. J Exp Bot **54:** 867–874

Shimazaki K, Doi M, Assmann SM, Kinoshita T (2007) Light regulation of stomatal movement. Annu Rev Plant Biol **58:** 219–247

Sutter JU, Sieben C, Hartel A, Eisenach C, Thiel G, Blatt MR (2007) Abscisic acid triggers the endocytosis of the Arabidopsis KAT1 K^+ channel and its recycling to the plasma membrane. Curr Biol **17:** 1396–1402

Tanaka Y, Sugano SS, Shimada T, Hara-Nishimura I (2013) Enhancement of leaf photosynthetic capacity through increased stomatal density in Arabidopsis. New Phytol **198:** 757–764

Tang M, Hu YX, Lin JX, Jin XB (2002) Developmental mechanism and distribution pattern of stomatal clusters in Begonia peltatifolia. Acta Bot Sin **44:** 384–390

UNESCO World Water Development Report (2015) The United Nations World Water Development Report 2015: Water for a Sustainable World. UNESCO, Paris

Wang Y, Blatt MR (2011) Anion channel sensitivity to cytosolic organic acids implicates a central role for oxaloacetate in integrating ion flux with metabolism in stomatal guard cells. Biochem J **439:** 161–170

Wang Y, Papanatsiou M, Eisenach C, Karnik R, Williams M, Hills A, Lew VL, Blatt MR (2012) Systems dynamic modeling of a guard cell Cl^- channel mutant uncovers an emergent homeostatic network regulating stomatal transpiration. Plant Physiol **160:** 1956–1967

Wilmer C, Fricker M (1996) Stomata. Chapman and Hall, London

Yang M, Sack FD (1995) The *too many mouths* and *four lips* mutations affect stomatal production in *Arabidopsis*. Plant Cell **7:** 2227–2239

Yoo CY, Pence HE, Jin JB, Miura K, Gosney MJ, Hasegawa PM, Mickelbart MV (2010) The *Arabidopsis* GTL1 transcription factor regulates water use efficiency and drought tolerance by modulating stomatal density via transrepression of SDD1. Plant Cell **22:** 4128–4141

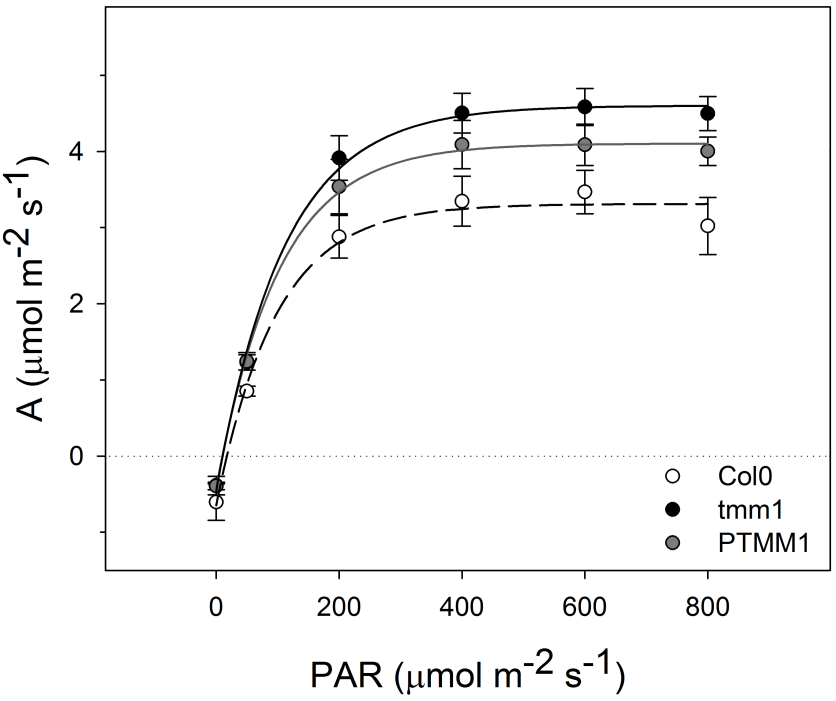

Suppl. Figure 1. Effect of photosynthetic active radiation on CO_2 assimilation.

Light curves from *Arabidopsis* plants grown under standard conditions display the assimilation of CO_2 over a range of PAR (from 0 to 800 µmol m^{-2} s^{-1}). Data were fitted to exponential rise curve and fittings are shown for *Arabidopsis* wild type (black dashed line), *tmm1* (black solid line) and PTMM1 (gray line). Data are means ±SE of n=3 plants.

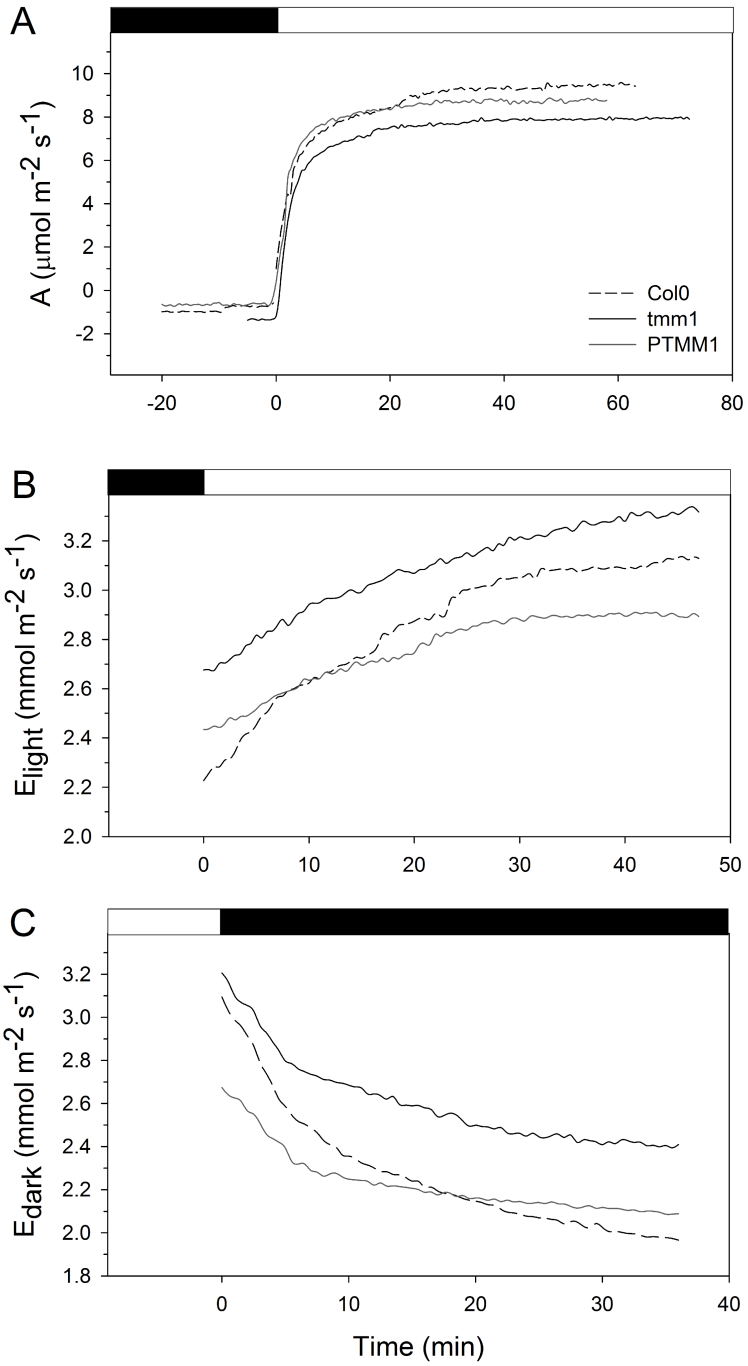

Suppl. Figure 2. Time-series of gas exchange responses from *Arabidopsis* plants.

Representative raw data of gas exchange responses were presented for *Arabidopsis* wild type (black dashed line), *tmm1* (black solid line) and PTMM1 (gray line) plants. Plant material was dark-adapted before treated with light of 400 µmol m^{-2} s^{-1} to measure CO_2 assimilation (A) and transpiration rate (B). Plants were subsequently exposed to darkness and transpiration rate was measured (C). Measurements were carried out with all other parameters held constant (390 ppm CO_2, 55% RH, 22°C).

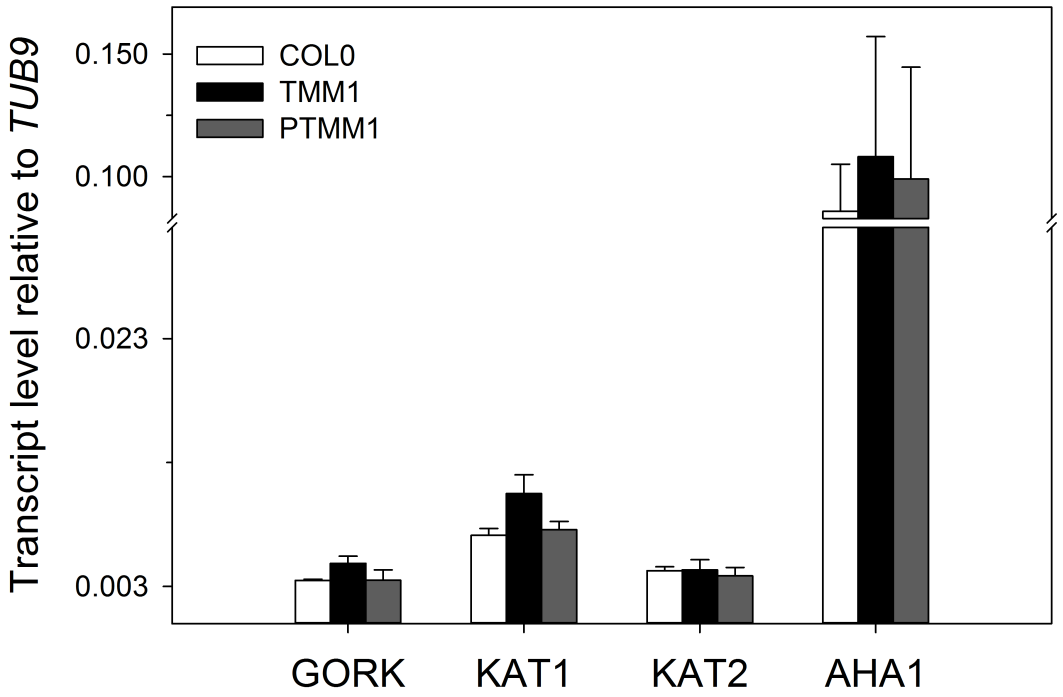

Suppl. Figure 3. Transcript level of major plasma membrane transport genes in *Arabidopsis* lines.

RNA extracted from leaves of three-week old *Arabidopsis* wild type (white), *tmm1* (black) and PTMM1 (dark gray) plants to perform quantitative PCR for genes encoding GORK, KAT1 and KAT2 ion channels and H^+-ATPase AHA1, using *TUB9* gene as constitutive control. Data are means ±SE of n=3 biological replicates. No statistical significant differences were detected after ANOVA ($P<0.05$).